PERGAMON

Available online at www.sciencedirect.com
SCIENCE DIRECT

Electrochimica Acta 48 (2003) 1023–1029

ELECTROCHIMICA Acta

www.elsevier.com/locate/electacta

The effect of cobalt oxide sintering aid on electronic transport in $Ce_{0.80}Gd_{0.20}O_{2-\delta}$ electrolyte

D.P. Fagg[a,*], J.C.C. Abrantes[b], D. Pérez-Coll[c], P. Núñez[c], V.V. Kharton[a], J.R. Frade[a]

[a] *Department of Ceramics and Glass Engineering, CICECO, University of Aveiro, 3810-193 Aveiro, Portugal*
[b] *ESTG, Instituto Politécnico de Viana do Castelo, 4900 Viana do Castelo, Portugal*
[c] *Departamento de Química Inorgánica, Universidad de La Laguna, E-38200 La Laguna, Tenerife, Spain*

Received 9 October 2002; received in revised form 9 December 2002

Abstract

Additions of 2 mol% $CoO_{1.333}$ into gadolinia-doped ceria (CGO) solid electrolyte considerably improve sinterability and make it possible to obtain $Ce_{0.8}Gd_{0.2}O_{2-\delta}$ ceramics with 95–99% density at 1173–1373 K. The effect of cobalt oxide on the total electrical conductivity in air is negligible if the sintering is performed at 1173 K, although p-type electronic conduction measured at 900–1200 K increases with doping by 10–30 times. When increasing the sintering temperature up to 1773 K, grain growth in Co-containing CGO ceramics is accompanied with a decrease in both ionic and electron-hole transport. The oxygen ion transference numbers under oxygen/air gradient vary in the range 0.89–0.99. The n-type conductivity measured by the ion-blocking technique is lower for Co-containing materials than for undoped CGO, suggesting that the electrolytic domain can, to some extent, be enlarged by cobalt oxide additions. The relative role of both p- and n-type electronic contributions to the total conductivity of CGO increases with increasing temperature. The results show that Co-doped materials can still be used as solid electrolyte for intermediate-temperature electrochemical applications, when the operation temperature is 770–970 K.

Keywords: Gadolinia-doped ceria; Solid electrolyte; Transference number; Electronic transport; Oxygen ionic conductor

1. Introduction

For application in electrochemical devices operating at intermediate temperatures (770–970 K), solid electrolytes based on doped cerium dioxide, $Ce(M)O_{2-\delta}$ (M: rare earth or alkaline earth cations), are considered to be one of the most promising alternatives to yttria stabilised zirconia (YSZ) as they offer four to five times higher ionic conductivity in this temperature range [1–7]. Successful incorporation in devices such as solid oxide fuel cells (SOFCs) has been demonstrated at temperatures below 1020 K when electronic leakage due to reduction of Ce^{4+} to Ce^{3+} is minimal. Interest in ceria-based electrolytes has been impeded, however, by poor mechanical strength, a problem notably undesirable for electrolyte-supported cells. The achievement of full density by conventional sintering methods requires high temperatures (up to 1870 K) resulting in the formation of microstructures with grain sizes in the micron range which subsequently offer poor mechanical stability [7,8]. Recently Kleinlogel and Gauckler [6,7] have sintered dense Gd-substituted CeO_2 (CGO) with nanosized grains at temperatures as low as 1173 K by the addition of small quantities (~2 mol%) of binary metal oxides such as cobalt oxide. The nanosized grain structure is likely to have greater mechanical stability than classically processed CGO sintered at higher temperatures. Negatively, additions of variable-valence cations, such as Co, might increase the p-type electronic conductivity of CGO. Results on the total conductivity of 2%Co-doped CGO as a function of oxygen partial pressure suggested that both the ionic conductivity and electrolytic domain at low $p(O_2)$ are essentially unaffected by the doping [7]. However, this type of measure-

---

[*] Corresponding author. Tel.: +351-234-370-263; fax: +351-234-425-300.
E-mail address: duncan@cv.ua.pt (D.P. Fagg).

0013-4686/02/$ - see front matter © 2002 Elsevier Science Ltd. All rights reserved.
doi:10.1016/S0013-4686(02)00816-2

ment is insufficient for a definite understanding of the electronic contribution to the total conductivity when predominantly ionic. Continuing our studies of ionic and electronic transport in CeO_2-based electrolytes [9–14], this work is focused on the determination of electronic conduction, both p- and n-types, in CGO ceramics containing 2 mol% $CoO_{1.333}$, using more precise techniques such as the modified electromotive force method and the ion blocking technique. Special attention is focused on the effects of sintering temperature, which may influence both grain size in the resultant materials and Co distribution between grain bulk and boundaries.

2. Experimental procedures

Commercial powder of $Ce_{0.80}Gd_{0.20}O_{2-\delta}$ (CGO), supplied by Rhodia GmbH (Frankfurt, FRG), with crystallite size of 20 nm and specific surface area of about 26 m^2/g was used as one starting material. To this powder 2 mol% cobalt oxide was added in the form of an aqueous solution of nitrate, $Co(NO_3)_2 \cdot 6H_2O$ (Merck KGaA, Darmstadt, FRG), with subsequent mixing, drying and thermal decomposition. The powder was milled in an agate mortar, and dry compacted into pellets (diameter of 20 mm, pressure of about 30 MPa) followed by isostatic pressing at 200 MPa. Sintering was performed in a regular furnace in air at various temperatures for 5 h, using heating/cooling rates of 10 K/min. Hereafter these materials are designated as 2%Co-CGO. Dense $Ce_{0.80}Gd_{0.20}O_{2-\delta}$ ceramics without cobalt oxide additions, used in this work for comparison, were sintered at 1773–1873 K; selected results of their characterisation can be found in [10–12].

The final density of the sintered materials was determined by the Archimedes method. Phase composition was determined by X-ray diffraction (XRD) using a Rigaku Geigerflex diffractometer (CuK$_\alpha$ radiation); the unit cell parameters were calculated with the program FULLPROF. No evidence of secondary phases was discernible by XRD; the observed phase was identified as cubic fluorite-type, similar to that of undoped CGO. Microstructural analysis was performed by scanning electron microscopy (SEM) on either fracture surfaces of ceramic samples or on polished samples thermally etched for 30 min at temperatures 100 K below that of the respective sintering temperature. Transmission electron microscopy (TEM) coupled with Energy dispersive analysis (EDS), using a Hitachi H9000-NA instrument, was carried out for powders obtained by crushing sintered ceramics to follow microstructural and compositional variations on the nano-scale level. Samples were supported on copper formvar grids by immersion in suspensions of crushed samples in absolute ethanol. Experimental procedures and equipment used for the measurements of total conductivity, transference numbers and partial ionic and electronic conductivities were reported elsewhere ([9–14] and references cited). The total conductivity was determined from ac impedance spectroscopic data using dense ceramic pellets. Trace electron-hole conductivity was separated from total electrical conductivity by the modified emf method first proposed by Gorelov [15]. This modification of the classical emf technique eliminates possible errors in the determination of ion transference numbers arising due to electrode polarisation, errors that are shown to be non-negligible for electrolyte-type materials which possess relatively minor electronic conductivity [11,16]. Description of the ion blocking technique, used to separate n-type conductivity, is found in [12].

3. Results and discussion

3.1. Microstructural characterisation

The density values and average grain sizes of materials, sintered in different conditions, are listed in Table 1. Sintering at 1173–1373 K for a sufficient time makes it possible to obtain 2%Co-CGO ceramics with 95–99% density, in agreement with [6,7]. At higher temperatures, a decrease in the density is observed. Representative examples of SEM micrographs of 2%Co-CGO materials are given in Fig. 1. For the samples produced at low temperature (1173 K), a fracture surface was analysed due to limits of resolution of the SEM technique for grain sizes less than 500 nm. Average grain size is in the range 100–200 nm, for samples sintered at 1173 K, and increases with sintering temperature up to 4–10 μm at 1773 K. Clear evidence of pores are visible for samples sintered at elevated temperatures, higher than 1373 K. Fig. 1 also presents a TEM micrograph of 2%Co-CGO ceramics sintered at 1773 K for 5 h. In the vicinity of the pore, distinct regions of inhomogeneity can be observed. EDS analysis reveals that these areas of inhomogeneity are highly Co rich in comparison to that of the bulk composition, Fig. 2. No compositional variations between bulk and grain boundary layers can be observed in samples sintered at 1773 K, in contrast to the data on materials sintered at 1173 K, in which EDS analysis suggested enrichment of boundary layers of CGO grains with transition metal oxide.

3.2. Total conductivity in air

Fig. 3 plots the low-temperature bulk conductivities of 2%-CGO ceramics sintered for 5 h at different temperatures. Bulk conductivities are shown to decrease with increasing sintering temperature. As sintering temperature increases a greater amount of Co dissolves into the CGO lattice, which leads to both decreasing

Table 1
Grain size and relative density of CeO_2-based ceramics sintered in various conditions

Material	Sintering temperature (K)	Sintering time (h)	Relative density (%)	Grain size (μm)
2%Co-CGO	1173	0.3	88.7±0.4	0.1–0.2
	1173	2	95.6±0.5	0.1–0.2
	1173	5	94.8±0.6	0.1–0.2
	1173	12	94.6±0.5	0.1–0.2
	1273	5	99.5±0.2	
	1373	5	99.4±0.3	0.3–0.5
	1573	5	95.0±0.6	
	1773	5	83.4±0.7	4–10
CGO	1873	6	96.4±0.5	1–8

ionic and increasing p-type electronic transport in the grain bulk [17]. Dissolution of Co cations in the ceria lattice results in a lower total conductivity of the ceramic grains, as the magnitude of the depletion of the ionic conductivity on cobalt dissolution is greater than the enhancement of electron-hole conduction [17]. Similar behaviour was observed for transition metal doped zirconia and for Mn-containing CGO [18–20]. Possible reasons for the decreasing ionic transport refer to oxygen vacancy association with relatively small cobalt cations, reflected by an increased apparent activation energy for conduction (Fig. 3). An increased concentration of aliovalent Co in the lattice, perhaps also coupled with an increasing vacancy concentration due to Co reduction at elevated temperature, can be suggested to increase the binding energy for dopant–vacancy association and to result in local lattice distortions near Co ions. Effects, associated with short-range ordering and decreasing mobility of oxygen ions are typical for most fluorite oxide phases doped with transition metal oxides (e.g. [18,21]). For the same 2%Co-CGO samples, Fig. 4 compares the values of the total conductivity (σ) measured at higher temperatures with that of undoped CGO ceramics. No significant change in total conductivity is observed for the material sintered at 1173 K, whilst slight decreases in the conductivity can be induced with increasing sintering temperature, analogous to that observed in Fig. 3.

3.3. Electron-hole conductivity

The ion transference numbers (t_o) measured by the modified emf technique under the oxygen partial pressure gradient of 101/21 kPa, are presented in Table 2. Decreasing temperature leads to smaller electron-hole contribution to the total conductivity, clearly indicating that the activation energy for the p-type conduction is higher than that for ionic transport. Combining trans-

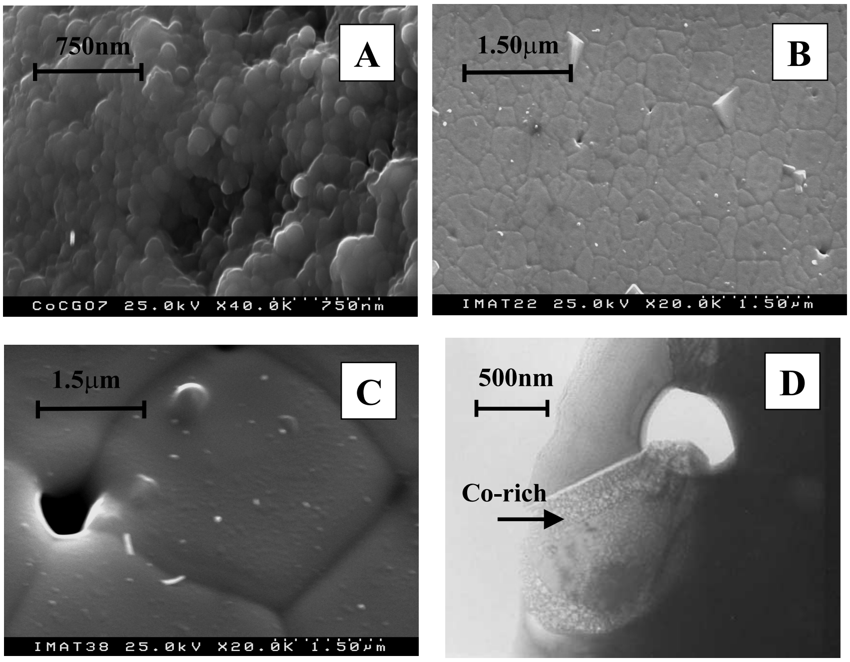

Fig. 1. (A, B and C) and TEM (D) micrographs of 2%Co-CGO sintered at (A) 1173 K for 2 h, (B) 1373 K for 5 h, (C) and (D) 1773 K for 5 h.

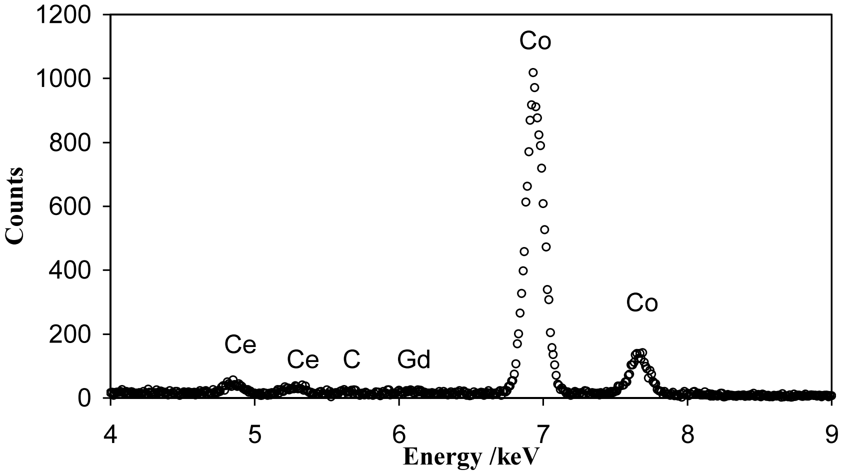

Fig. 2. TEM/EDS spectrum of an inhomogeneous region of 2%Co-CGO ceramics sintered at 1773K for 5 h.

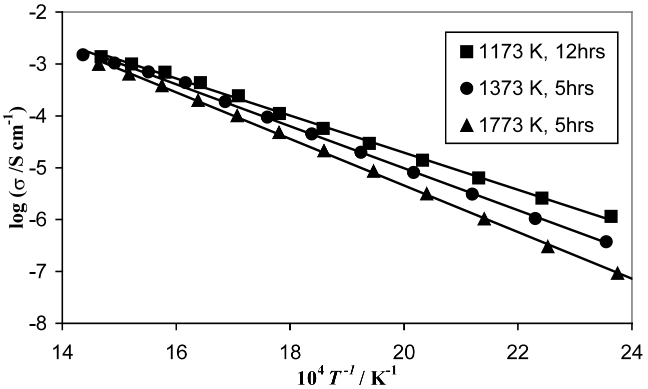

Fig. 3. Temperature dependence of bulk contributions to total conductivity in air, separated by a.c. impedance spectroscopy for 2%Co-CGO sintered at different temperatures for 5 h.

ference numbers with σ values obtained by impedance spectroscopy allows p-type electronic conductivity to be estimated as $\sigma_p = (1 - t_o)\sigma$ In oxidising conditions the n-type contribution is extremely small [1,10,12] and was thus neglected. Fig. 5 presents the p-type conductivity values of 2%Co-CGO ceramics compared with that of undoped CGO. The presence of 2% cobalt oxide leads to elevated p-type conductivity for every sintering temperature. For 2%Co-CGO sintered at 1173 or 1373 K an enhancement of over 1.5 orders of magnitude is exhibited with respect to that of the undoped CGO material. Table 3 lists the activation energy (E_a) values for the p-type electronic and ionic conductivities, calculated by the standard Arrhenius equation:

$$\sigma = \frac{A_0}{T} \exp\left[-\frac{E_a}{RT}\right] \qquad (1)$$

where, A_0 is the pre-exponential factor. While 2%Co-CGO ceramics sintered at 1173–1373 K exhibit similar p-type conductivity, sintering at 1773 K leads to significantly lower σ_p values.

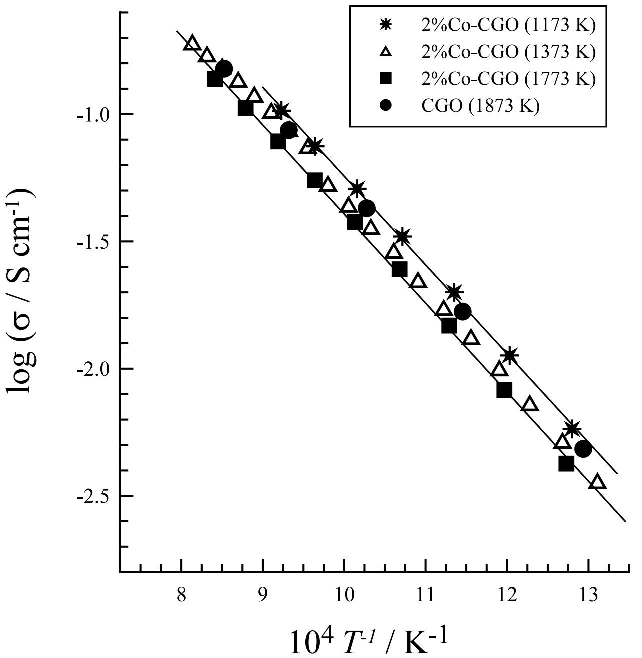

Fig. 4. Temperature dependence of the total conductivity of Co-containing CGO ceramics, sintered at different temperatures, in air.

When analysing transport properties of Co-containing CGO as a function of processing conditions, one should take into account the data on similar systems with fluorite-type oxide structure: ZrO_2-based materials doped with transition metal oxides [18,20,21], Co- and Mn-doped $Ce(Gd)O_{2-\delta}$ sintered at high temperatures [17,19], and Co-doped $Bi(Y)O_{1.5-\delta}$ [22]. These data unambiguously show that dissolution of transition metal cations into the lattice leads to a weakly enhanced p-type lattice conductivity and to a moderate decrease in ionic transport. In the case of the studied materials, EDS analysis of materials sintered at 1173 K suggests enrichment of the boundary layers of the CGO grains with transition metal oxide. For samples sintered at 1773 K, no such compositional variations between bulk

Table 2
Oxygen ion transference numbers of 2%Co-CGO ceramics, sintered at different temperatures for 5 h, under the oxygen/air gradient

Sintering temperature (K)	T (K)					
	923	973	1023	1073	1123	1173
1173	0.98	0.97	0.95	0.93	0.90	0.89
1373	0.97	0.96	0.93	0.92	0.91	0.89
1773	–	0.99	0.99	0.98	0.98	0.97

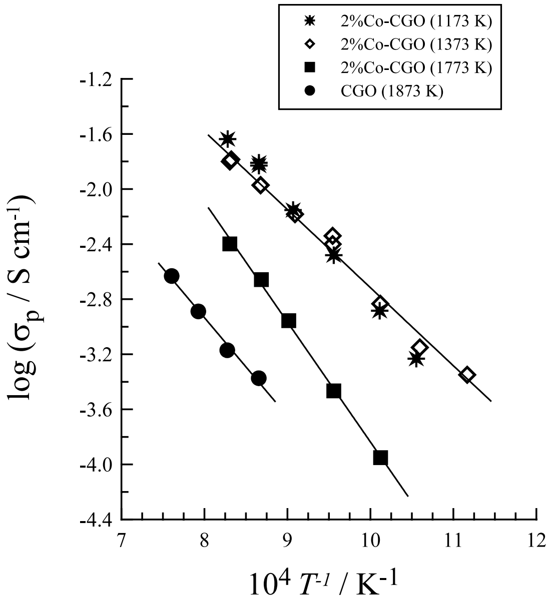

Fig. 5. Temperature dependence of the p-type electronic conductivity of 2%Co-CGO ceramics sintered for 5 h at different temperatures, calculated from the results on the total conductivity and transference numbers under the oxygen/air gradient.

and grain boundary layers are observed, whereas some cobalt oxide is segregated to regions of ceramic flaw. The variation in p-type conductivity observed for the 2%Co-CGO compositions sintered at different temperatures may, therefore, result from two distinct phenomena. The first phenomenon relates to that suggested in previous works [17–22], in which one would propose a change in electron-hole conduction pathway from along Co-rich grain boundary layers to lattice p-type transport due to a greater amount of Co being dissolved into the bulk as sintering temperature increases. This is accompanied with lower ionic conduction, as reflected by the observed decrease in the total conductivity (Figs. 3 and 4). Alternatively, initiating from the EDS analysis in this work, one could also suggest that segregation of Co has led to a break in Co-rich boundary layer conducting networks and subsequently increased activation energy for the hole conduction in materials sintered at higher temperatures. It should be noted that consensus of the solubility limit of Co in CGO still has not been reached in literature, varying from 0.5–2 mol% [23,24] up to 10–30 mol% [17,25]. The observation that some Co is segregating in 2%Co-CGO ceramics, sintered at 1773 K, perhaps reinforces the latter argument.

Finally, the ion transference numbers of Co-containing CGO under oxygen/air gradient are 0.89–0.97 at 1173 K, but increase to 0.96–0.99 when temperature decreases to 973 K (Table 2). Hence, in order to avoid performance losses, the use of these materials as solid electrolytes in oxidising conditions should be limited by the temperature range 773–973 K.

3.4. *n-type electronic transport*

The n-type conductivity can be extracted from the dependence of the electronic current density (J_e) on voltage (V_0) under steady state ion-blocking conditions [26–29]. A generic analytical solution has been proposed on assuming that the total electronic conductivity (σ_e) is:

$$\sigma_e = \sigma_p + \sigma_n = \sigma_p^0 \cdot [p(O_2)]^{1/4} + \sigma_n^0 \cdot [p(O_2)]^{-1/4} \qquad (2)$$

Table 3
Regression parameters of the Arrhenius model for the partial ionic and p-type electronic conductivities of $Ce_{0.8}Gd_{0.2}O_{2-\delta}$ and 2%Co-CGO ceramics sintered at different temperatures, in air

Composition and sintering temperature	Conductivity	T (K)	E_a (kJ/mol)	ln A_0 (S*K/cm)
2%Co-CGO (1173 K)	Ionic	630–1090	79±1	13.6±0.2
	p-type electronic	920–1180	146±3	18.4±0.4
2%Co-CGO (1373 K)	Ionic	730–1100	76.9±0.5	13.1±0.1
	p-type electronic	870–1180	118±5	15.2±0.5
2%Co-CGO (1773 K)	Ionic	580–1090	79.2±0.7	13.2±0.1
	p-type electronic	970–1170	176±6	19.7±0.5
$Ce_{0.8}Gd_{0.2}O_{2-\delta}$ (1873 K)	Ionic	720–1270	72.9±0.8	12.7±0.1
	p-type electronic	1070–1270	145±8	14.8±0.8

where, σ_n is the n-type electronic conductivity, and the quantities σ_n^0 and σ_p^0 represents the corresponding contributions at unit oxygen partial pressure, $p(O_2)$. In this case [27–29]:

$$J_e = \frac{RT}{FL}\left\{\sigma_n^0 \cdot \left[\exp\left(\frac{V_0F}{RT}\right) - 1\right] + \sigma_p^0 \cdot \left[1 - \exp\left(-\frac{V_0F}{RT}\right)\right]\right\} \quad (3)$$

where L is the thickness of the sample. However, this solution cannot describe the transition from the (−1/4) power law to other types of dependence expected under very reducing conditions, e.g. the (−1/6) power law. More reliable results in a wide $p(O_2)$ range can, therefore, be obtained using the original differential equation [29]:

$$\sigma_e(V_0) = L\frac{dJ_e}{dV} \quad (4)$$

In this case, the dependence of current density on voltage should be differentiated numerically to obtain the voltage dependence of total electronic conductivity. The main advantage of this method is that experimental data are analysed without imposing any type of dependence of the n- and/or p-type contributions on oxygen partial pressure [29]. When $p(O_2)$ at the reversible reference electrode is fixed at p^{ref}, the quantity σ_n relates to the blocking electrode, where the oxygen pressure can be estimated using Nernst law:

$$p(O_2) = p^{\text{ref}} \cdot \exp\left(-\frac{4FV_0}{RT}\right) \quad (5)$$

On combining Eqs. 4 and 5 one thus obtains the $p(O_2)$ dependence of electronic conductivity.

Selected experimental results are shown in Fig. 6 for one CGO sample sintered at 1773 K without cobalt additive (dashed lines), and also for a 2%Co-containing sample fired at 1423 K (solid line). The addition of Co clearly displaces the onset of significant electronic current density. These data were numerically differentiated to obtain the σ_e versus V_0 dependence (Eq. 4); Eq. 5 was used to derive the corresponding values of the oxygen partial pressure.

The results shown in Fig. 7 confirm that the onset of the electronic conductivity is displaced towards more reducing conditions in Co-containing materials. Such a change is consistent with the corresponding enhancement of the p-type contribution measured under oxidising conditions (see Section 3.3). In fact, the concentration of electrons should increase with decreasing concentration of electron holes, as predicted by the mass action law of the intrinsic thermal generation of electronic defects. A line with slope (−1/6) is shown to emphasise the deviations from a simple (−1/4) power law.

Typical values of electronic conductivity are also shown in Table 4 for oxygen chemical potentials, characteristic of SOFC anode operation (wet H_2 or converted hydrocarbons). For example, gas mixtures with H_2O:H_2 ratio in the range of 1–5 yield values of $p(O_2)$ in the range of 10^{-16}–10^{-18} at 1073 K, about 10^{-14}–10^{-16} at 1173 K, and about 10^{-12}–10^{-14} at 1273 K. On combining the values of electronic conductivity with the corresponding ionic conductivity, one obtains electron transference numbers (t_e) also shown in Table 4. The values of electronic transport number have been significantly lowered in the material with cobalt oxide addition. This effect exceeds the slightly negative effect of increasing electron-hole conductivity under oxidising conditions (Fig. 5), mainly because the ion transference numbers in air remain close to unity (Table 2).

4. Conclusions

Doping of $Ce_{0.8}Gd_{0.2}O_{2-\delta}$ solid electrolyte with 2 mol% cobalt oxide has no effect on the total conductivity if sintering is performed at 1173–1273 K. Further increases in sintering temperature results in increasing grain size, decreasing density and lower total conductivity values. Although the additions are small, the p-type

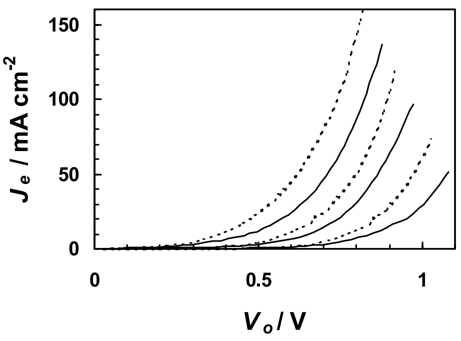

Fig. 6. Ion blocking results obtained for CGO with 2 mol% cobalt oxide addition (solid lines), and CGO without Co additions (dashed lines), at 1273 K, 1173 K and 1073 K (from left to right).

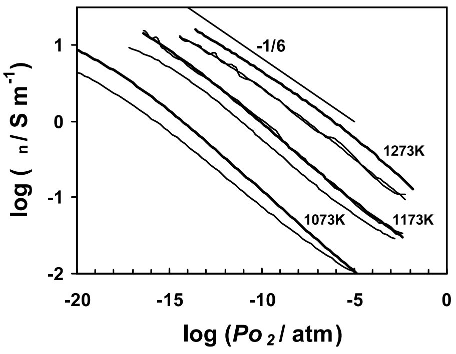

Fig. 7. n-type electronic conductivity of CGO with 2 mol% cobalt oxide addition (thin solid lines), and CGO without Co additions (thick solid lines), at 1073 K, 1173 K and 1273 K (from left to right).

Table 4
n-type electronic conductivity and electron transference numbers for 2%Co-CGO ceramics fired at 1423K and $Ce_{0.8}Gd_{0.2}O_{2-\delta}$ ceramics fired at 1773 K under typical values of $p(O_2)$ in wet H_2

Composition and sintering temperature	T (K)	$p(O_2)$ (atm)	n-type conductivity $\sigma_n \times 10^2$ (S/cm)	Electron transport number, t_e
2% Co-CGO (1423 K)	1073	10^{-16}	1.07	0.12
		10^{-18}	2.15	0.21
	1173	10^{-14}	3.38	0.18
		10^{-16}	6.80	0.30
	1273	10^{-12}	5.80	0.18
		10^{-14}	11.4	0.30
CGO (1773 K)	1073	10^{-16}	2.07	0.19
		10^{-18}	4.50	0.34
	1173	10^{-14}	5.38	0.25
		10^{-16}	12.9	0.45
	1273	10^{-12}	8.42	0.24
		10^{-14}	19.1	0.42

conductivity of ceria-based ceramics significantly increases on doping. The oxygen ion transference numbers of Co-containing materials, determined by the modified emf method at 923-1173 K under an oxygen/air gradient, vary in the range from 0.89 to 0.99, decreasing when temperature increases. At high sintering temperatures, such as 1773 K, electron-hole transport in Co-doped CGO ceramics becomes lower and possesses higher activation energy. The n-type conductivity of Co-containing ceria, and the corresponding electron transference numbers are considerably lower than those for undoped ceramics. This effect thus contributes to extend the electrolytic domain of Co-doped $Ce_{0.8}Gd_{0.2}O_{2-\delta}$, and enhances their potential application in intermediate-temperature electrochemical cells.

Acknowledgements

This work was supported by the FCT, Portugal (PRAXIS and POCTI programs and the contract SFRH/BPD/3529/2000) and Spanish Research Program (MCYT MAT2001-3334). One of the authors (DPC) wishes to thank OSSEP-ESF and Cajacanarias-ULL Program for financial support.

References

[1] B.C.H. Steele, Solid State Ionics 129 (2000) 95.
[2] J.P.P. Huijsmans, Curr. Opin. Solid State Mater. Sci. 5 (2001) 317.
[3] O. Yamamoto, Electrochim. Acta 45 (2000) 2423.
[4] G.M. Christie, F.P.F. van Berkel, Solid State Ionics 83 (1996) 17.
[5] S.J. Hong, K. Mehta, A.V. Virkar, J. Electrochem. Soc. 145 (1998) 638.
[6] C. Kleinlogel, L.J. Gaukler, in: S.C. Singhal, M. Dokiya (eds.), SOFC VI, The Electrochemical Society, Pennington, 1999, PV 99-19, pp. 225.
[7] C. Kleinlogel, L.J. Gauckler, Solid State Ionics 135 (2000) 567.
[8] A. Atkinson, A. Selcuk, in: U. Stimming, S.C. Singhal, H. Tagawa, W. Lehnert (eds.), SOFC V, The Electrochemical Society, Pennington, 1997, PV 97-40, pp. 671.
[9] V.V. Kharton, A.P. Viskup, F.M. Figueiredo, E.N. Naumovich, A.L. Shaulo, F.M.B. Marques, Mater. Lett. 53 (2002) 160.
[10] V.V. Kharton, F.M. Figueiredo, L. Navarro, E.N. Naumovich, A.V. Kovalevsky, A.A. Yaremchenko, A.P. Viskup, A. Carneiro, F.M.B. Marques, J.R. Frade, J. Mater. Sci. 36 (2001) 1105.
[11] V.V. Kharton, A.P. Viskup, F.M. Figueiredo, E.N. Naumovich, A.A. Yaremchenko, F.M.B. Marques, Electrochim. Acta 46 (2001) 2879.
[12] L.M. Navarro, F.M.B. Marques, J.R. Frade, J. Electrochem. Soc. 144 (1997) 267.
[13] G.C. Mather, D.P. Fagg, A. Ringuedé, J.R. Frade, Fuel Cells 1 (2001) 233.
[14] D.P. Fagg, J.R. Frade, V.V. Kharton, J. Electroceramics, submitted (2002).
[15] V.P. Gorelov, Elektrokhimiya 24 (1988) 1380 (in Russian).
[16] V.V. Kharton, F.M.B. Marques, Solid State Ionics 140 (2001) 381.
[17] A.V. Kovalevsky, V.V. Kharton, E.N. Naumovich, Inorg. Mater. 32 (1996) 1230.
[18] V.V. Kharton, E.N. Naumovich, A.A. Vecher, J. Solid State Electrochem. 3 (1999) 61.
[19] V.V. Kharton, A.V. Kovalevsky, A.P. Viskup, F.M. Figueiredo, A.A. Yaremchenko, E.N. Naumovich, F.M.B. Marques, J. Electrochem. Soc. 147 (2000) 2814.
[20] J.H. Kim, G.M. Choi, Solid State Ionics 130 (2000) 157.
[21] L.S.M. Traqueia, T. Pagnier, F.M.B. Marques, J. Eur. Ceram. Soc. 17 (1997) 1019.
[22] V. Kharton, E. Naumovich, V. Samokhval, Solid State Ionics 99 (1997) 269.
[23] J.D. Sirman, D. Waller, J.A. Kilner, in: W.L. Worrell (ed.), Ionic and Mixed Conducting Ceramics III, The Electrochemical Society, Pennington, 1998, PV 97-24, pp. 1159.
[24] J. Ranløv, F.W. Poulsen, M. Mogensen, Solid State Ionics 61 (1993) 277.
[25] G. Dontsov, G. Vitter, C. Déportes, Rev. Int. Hautes Tempér. Réfract. 9 (1972) 147.
[26] M. Hebb, J. Chem. Phys. 20 (1952) 185.
[27] C. Wagner, in: Proceedings of 7th Meeting of International Community on Electrochemical Thermodynamics and Kinetics, Butterworths, London, 1957, pp. 361.
[28] R.M.C. Marques, F.M.B. Marques, J.R. Frade, Solid State Ionics 73 (1994) 15.
[29] R.M.C. Marques, F.M.B. Marques, J.R. Frade, Solid State Ionics 73 (1994) 27.